Reports

Multiple Light-Scattering Probes of Foam Structure and Dynamics

D. J. DURIAN, D. A. WEITZ, D. J. PINE

The structure and dynamics of three-dimensional foams are probed quantitatively by exploiting the strong multiple scattering of light that gives foams their familiar white color. Approximating the propagation of light as a diffusion process, transmission measurements provide a direct probe of the average bubble size. A model for dynamic light scattering is developed that can be used to interpret temporal fluctuations in the intensity of multiply scattered light. The results identify previously unrecognized internal dynamics of the foam bubbles. These light-scattering techniques are direct, noninvasive probes of bulk foams and therefore should find wide use in the study of their properties.

FOAM IS A RANDOM DISPERSION OF gas bubbles separated by thin liquid films. Foams have a myriad of important uses, from smothering fires, containing explosions, and trapping toxic materials to dying garments, enhancing oil recovery, and shaving (*1*). In addition, foams are of broad scientific interest for their ability to efficiently fill space with a random packing of bubbles and for the coarsening of this disordered structure with age (*2–4*). However, neither the fundamental origin of the unique rheological behavior of foams nor the physical mechanisms that affect their stability are well understood. In part, this is due to the fact that the structure, distribution, and dynamics of foam bubbles remain largely inaccessible to traditional experimental measurements such as surface observation, freeze fracture, electrical conductivity, or external pressure (*4*). Furthermore, the strong scattering of light, which gives foams their familiar white appearance, precludes direct visualization of these key features.

In this report, we exploit this multiple light scattering to develop quantitative probes of both the structure and the internal dynamics of foam. First, we show that the time-averaged transmission of light through foam yields a simple, yet quantitative, measure of the average bubble size. Second, we develop a model of dynamic light scattering for analyzing the time-dependent fluctuations in the scattered light intensity and discover an important dynamic process in the foam. In earlier studies of light transmission it was assumed that foam can be modeled as periodic layers of liquid and gas (*5*). Here, we take a completely different approach, assuming only that the propagation of multiply scattered light can be described as a diffusion process.

We used a commercial foam to provide convenient and reproducible experimental samples (*6*). The essential ingredients, water and surfactants pressurized with hydrocarbon gases, produce a foam with 92 ± 1% gas by volume. A typical photograph of the surface of this foam (Fig. 1A) exhibits a random packing of nearly spherical bubbles. The average diameter is initially 20 μm and grows to 200 μm in 1 day as the foam coarsens by diffusion of gas from smaller to larger bubbles. The change in the volume fraction owing to gravitational drainage of clear, slightly yellow liquid becomes significant only after about 3 days.

One of the simplest optical quantities to measure is the static transmission T of light through a thickness L of foam. We find that T increases with age, as the average bubble size grows. The L dependence is shown for foams of several ages in the logarithmic plot in Fig. 2. In contrast to the exponential dependence typical of absorbing or weakly scattering media, our data are consistent with the $T \sim 1/L$ dependence shown by the dashed line in Fig. 2. This dependence is a classic signature of diffusive light propagation. Supporting evidence is provided by the observation that the transmitted light is completely depolarized.

Diffusion of light is characterized by the transport mean free path, ℓ^*, the average distance a photon travels before its direction is randomized. Its value is defined by the diffusion coefficient for light, $v\ell^*/3$, where v is the speed of light in the medium (7). If we include an absorption length $\ell_a \gg \ell^*$, the solution of the diffusion equation for light gives (7)

$$T \approx \frac{(5\,\ell^*/3L)\beta}{[1 + (4\ell^*/3L)]\sinh\beta} \qquad (1)$$

$$\text{with } \beta = \sqrt{\frac{3L^2}{\ell^*\ell_a}}$$

In the limit of large L and no absorption ($L \gg \ell^*$ and $\beta \ll 1$), this reduces to $T \approx 5\ell^*/3L$. Experimental values of T are normalized by the relative transmission through an aqueous suspension of polystyrene latex spheres whose ℓ^* is accurately known from Mie theory (*8*). Our data are well described by Eq. 1, as shown by the solid curves in Fig. 2. We obtained these fits by adjusting ℓ^* and using $\ell_a = 200$ cm, determined by correcting the absorption

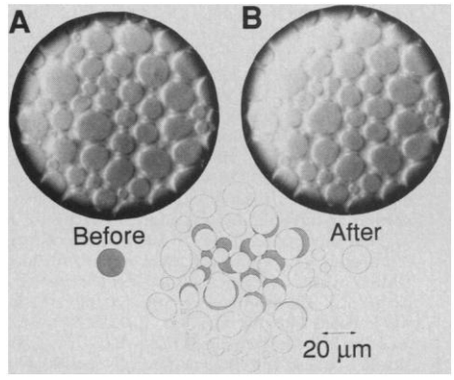

Fig. 1. Photographs of the foam surface against glass (**A**) before and (**B**) after a rearrangement event. The inset is a guide to the bubble movement. The time interval between photographs was 0.5 s, and the foam age was 1 min.

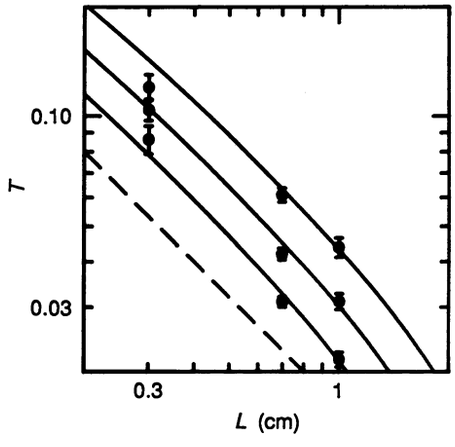

Fig. 2. Transmission versus foam thickness at 40, 90, and 200 min of age for wavelength λ = 488.0 nm; error bars are ± 1 standard deviation based on 10 to 50 measurements. With increasing age, more light is transmitted. The dashed line shows the form of $T \propto 1/L$. The solid curves are the best fits to Eq. 1.

Exxon Research and Engineering Company, Clinton Township, Route 22 East, Annandale, NJ 08801.

measured in the drained liquid for its volume fraction in the foam. The fits are insensitive to variation of ℓ_a by a factor of 2.

The length ℓ^* must reflect the foam structure. Provided that this structure can be parameterized by a single length scale, such as the average bubble diameter d (*9*) and provided that d is much greater than the wavelength of light, we expect that $\ell^* \propto d$. To test this, we compare in Fig. 3 values of ℓ^* measured from static transmission with estimates of d obtained by viewing surface bubbles. The nearly linear relation observed supports the assumption that a single length scale parameterizes the foam structure. For values of d between 40 and 200 μm, the relation $\ell^* = (3.5 \pm 0.5)d$ allows us to use ℓ^* as a measure of d (*10*). Furthermore, the value of ℓ^*/d is consistent with a geometric optics picture of light specularly reflecting from randomly oriented gas-liquid interfaces so that passage through several bubbles is required for full randomization of the light propagation.

Static transmission of light is a simple, noninvasive experiment, and analysis in terms of diffusive propagation yields a direct, quantitative measure of the average bubble size in a three-dimensional foam. Studying the coarsening of our foam, we find that ℓ^*, and hence the average bubble size, grows with time as t^z, where $z = 0.45 \pm 0.05$ (*10, 11*). Our results are consistent with $t^{1/2}$, as expected from mean-field theories (*9*).

The diffusive propagation of light aids in the analysis of not only the time average of the scattered light intensity but also its temporal fluctuations. The formalism of diffusing wave spectroscopy (DWS) (*12, 13*) can be used to interpret these fluctuations in terms of the underlying motion inside the foam. As in traditional dynamic light scattering (*14*), we illuminate the sample with a laser and arrange a pinhole and photomultiplier tube to observe a few speckles of the scattered light. A digital correlator computes the temporal intensity correlation function, from which the normalized field correlation function $g_1(\tau)$ is obtained (*14*).

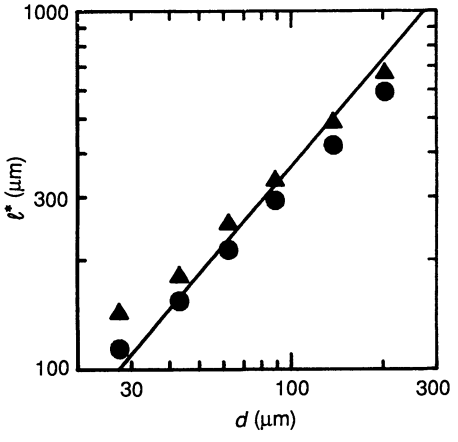

Fig. 3. Transport mean free path of light versus the average bubble diameter; we estimated the latter by viewing surface bubbles with a microscope. The static transmission results (●) agree with the dynamic measurements (▲) to within a slight systematic discrepancy. The solid line is the best fit to $\ell^* \propto d$.

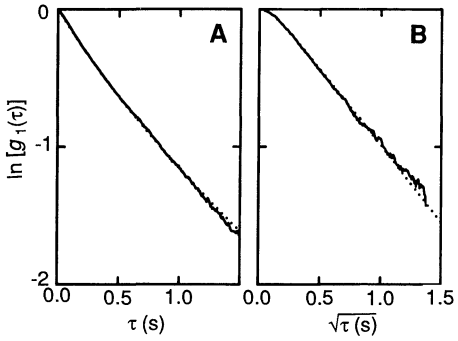

Fig. 4. Normalized field autocorrelation functions for light (**A**) transmitted through a 0.3-cm-thick cell and (**B**) backscattered from a 1-cm-thick cell. Data were collected for 10 min when the foam age was 100 min. The dotted curves are fits to Eqs. 3 and 2, respectively.

In Fig. 4, we show typical data collected when the foam had aged 100 min. The shape of $g_1(\tau)$ for transmitted light is nearly exponential in τ, whereas the shape for backscattered light is nearly exponential in $\sqrt{\tau}$. These shapes are identical to those obtained for diffusing Brownian particles, despite the absence of any such motion in the foam. In the limit of large L and no absorption, expressions for $g_1(\tau)$ in backscattering and transmission are, respectively (*13*),

$$g_{1,B}(\tau) \approx \exp[-2(6\tau/\tau_0)^{1/2}] \qquad (2)$$

and

$$g_{1,T}(\tau) \approx \frac{\sqrt{6\Gamma_1\tau}}{\sinh(\sqrt{6\Gamma_1\tau})},$$

$$\text{with } \Gamma_1 = \left(\frac{L}{\ell^*}\right)^2 \frac{1}{\tau_0} \qquad (3)$$

The time τ_0 reflects the effect of the internal foam dynamics on the light scattering (*13*). From the backscattering data, we find that τ_0 varies from 8 s initially to 120 s after 24 hours. We analyze the transmission data by its initial logarithmic slope, Γ_1 (*15*); from its L dependence we determine ℓ^*, using $\ell_a = 200$ cm and the τ_0 obtained from backscattering. The results shown in Fig. 3 (▲) agree with the values of ℓ^* obtained from static transmission (●), providing a stringent consistency check on our procedures.

A physical interpretation of τ_0 requires both the identification of the nature of the internal dynamics and the development of a model for the resultant temporal fluctuations in the scattered light. An essential feature of our data is the shapes of the correlation functions, which are described by Eqs. 2 and 3. These expressions were derived (*13*) by summing over diffusive paths of different lengths

$$g_1(\tau) = \int_0^\infty P(s) g_1^s(\tau) ds \qquad (4)$$

$P(s)$ is the fraction of paths with length s, and their contribution to the total decay is

$$g_1^s(\tau) = \exp[-2(\tau/\tau_0)(s/\ell^*)] \qquad (5)$$

The $g_1(\tau)$ data require that Eq. 5 be exponential in τs. This rules out contributions from capillary waves on bubble walls and from the coarsening of foam bubbles, because in either case the motions are correlated in time and would lead to very different shapes for $g_1(\tau)$. These processes can also be eliminated on the basis of time scales, capillary waves being too fast and coarsening waves being too slow. In addition, Brownian motion of the bubbles themselves is ruled out because of the strong mutual repulsion of neighboring bubbles.

Extended observation of the foam surface with a microscope revealed the nature of the dynamics. Initial examination typically shows a distribution of nearly spherical bubbles that appears static. However, continuous observation reveals dynamic processes of the sort illustrated by the sequence of photographs in Fig. 1. During the 0.5-s interval between these pictures, several bubbles underwent the structural rearrangement illustrated schematically in the inset. Similar rearrangements presumably occur throughout the whole foam. This motion does not result from the rupture of liquid films, because bubble coalescence is never observed. These rearrangement events differ from the rare "T1" neighbor-switching process (*16, 17*) of two-dimensional polyhedral foams in that they occur on a time scale short as compared to that of coarsening, and they do not serve to alter the bubble size distribution.

The bubble rearrangements cause fluctuations in the intensity of the scattered light; to analyze these we must construct a model for $g_1^s(\tau)$. Physically, the decay of $g_1^s(\tau)$ reflects the temporal randomization of the phases of the diffusive light paths of length s. For Brownian particles, randomization is caused by the constant temporal evolution of the path lengths due to the particle motion, and $g_1^s(\tau)$ is given by Eq. 5 (*12, 13*). For the foam, by contrast, we can assume that the length, and hence the phase, of any diffusive light path is constant in time until a rearrangement event occurs along the path,

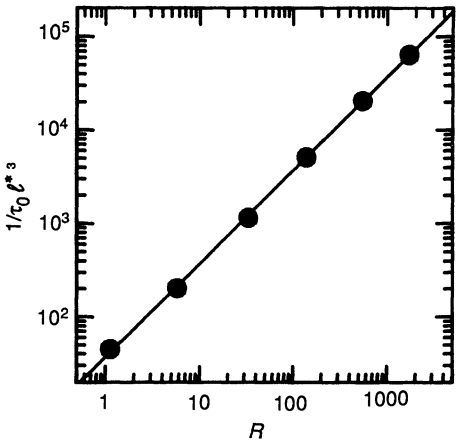

Fig. 5. The quantity $1/\tau_0\ell^{*3}$ versus the rate of rearrangement events per unit volume; we estimated the latter by viewing surface bubbles with a microscope. Both quantities are in units of s^{-1} cm^{-3}. The solid line is the best fit to $1/\tau_0\ell^{*3} \propto R$.

whereupon its length is suddenly changed and the phase is totally randomized. Thus, $g_1^s(\tau)$ is an ensemble average of the fraction of paths of length s that have not been randomized since time $\tau = 0$. If rearrangement events of a single size r occur randomly at rate R per unit volume, then $g_1^s(\tau) = e^{-\gamma_s\tau}$. The decay rate γ_s depends on the likelihood of a rearrangement event occurring within the path and so increases with the product of R and the path volume, $s\ell^{*2}$, where ℓ^* is the shortest meaningful length scale for a diffusive light path. Also, γ_s must increase with r^3/ℓ^{*3}, because larger events will affect more light paths. We therefore have $\gamma_s \approx R(s\ell^{*2})(r^3/\ell^{*3})$; comparison with Eq. 5 gives $\tau_0^{-1} \approx Rr^3$. Physically, τ_0 reflects the average time interval between rearrangement events at any single location in the foam.

To test this model, in Fig. 5 we compare $1/\tau_0\ell^{*3}$, measured by DWS, with R, estimated from the rate of rearrangements at the foam surface. Provided the average event size r scales with bubble size, our model predicts $1/\tau_0\ell^{*3} \propto R$. As the foam ages, both quantities decrease by many orders of magnitude, and Fig. 5 demonstrates a linear relation over the full range. The result, $1/\tau_0\ell^{*3} = (35 \pm 10)R$ (*10*), implies that the average event size scales with bubble size and is on the order of ten bubbles in diameter. This is in excellent agreement with our microscope observations of r, confirming the validity of our model for DWS.

In contrast to traditional dynamic light-scattering techniques, which probe continuous random movements, this form of DWS probes events that are temporally intermittent, large in scale, and spatially localized. Studying the time evolution of the foam, we find that $R \sim t^{-\gamma}$ with $\gamma = 2.0 \pm 0.1$ (*10, 11*). The origin, scaling behavior, and consequences of these rearrangement events have not yet been considered. Presumably, as the foam coarsens and packing conditions change, local stress differences accumulate until a critical value is reached and a rearrangement event occurs. This process must also play an essential role in the relaxation of applied stresses and therefore should provide important microscopic information about the macroscopic rheological behavior of foams. In general, rearrangement events may vary considerably with the nature of the foam, particularly with the volume fraction of liquid and with the prevalence of bubble coalescence. However, the simplicity and convenience of these multiple light-scattering techniques should enable these and other important fundamental properties of a wide variety of foams to be studied.

REFERENCES AND NOTES

1. J. H. Aubert, A. M. Kraynik, P. B. Rand, *Sci. Am.* **254**, 74 (May 1986).
2. A. J. Wilson, Ed., *Foams: Physics, Chemistry, and Structure* (Springer-Verlag, New York, 1989).
3. H. C. Cheng and T. E. Natan, in *Encyclopedia of Fluid Mechanics*, vol. 3, *Gas Liquid Flow*, N. P. Cheremisinoff, Ed. (Gulf, Houston, 1986).
4. A. M. Kraynik, *Annu. Rev. Fluid Mech.* **20**, 325 (1988).
5. N. O. Clark and M. Blackman, *Trans. Faraday Soc.* **44**, 7 (1948); S. Ross and M. J. Cutillas, *J. Phys. Chem.* **59**, 863 (1955).
6. Gillette Foamy Regular (Gillette Company, Box 61, Boston, MA 02199).
7. A. Ishimaru, *Wave Propagation and Scattering in Random Media* (Academic Press, New York, 1978), vol. 1.
8. P. E. Wolf, G. Maret, E. Akkermans, R. Maynard, *J. Phys. (Paris)* **49**, 63 (1988).
9. W. W. Mullins, *J. Appl. Phys.* **59**, 1341 (1986).
10. The quoted error reflects our estimate of the systematic uncertainties in the light-scattering measurements and in the estimate of bulk foam properties obtained by viewing surface bubbles.
11. D. J. Durian, D. A. Weitz, D. J. Pine, in preparation.
12. G. Maret and P. E. Wolf, *Z. Phys. B* **65**, 409 (1987).
13. D. J. Pine, D. A. Weitz, J. X. Zhu, E. Herbolzheimer, *J. Phys. (Paris)* **51**, 2101 (1990).
14. B. J. Berne and R. Pecora, *Dynamic Light Scattering: With Applications to Chemistry, Biology, and Physics* (Wiley, New York, 1976).
15. We generalize equation 3.5 of (*13*) to include the effect of absorption.
16. D. Weire and N. Rivier, *Contemp. Phys.* **25**, 59 (1984).
17. J. A. Glazier, S. P. Gross, J. Stavans, *Phys. Rev. A* **36**, 306 (1987).

18. We thank T. A. Witten and P. M. Chaikin for suggestions and the deckmen for their help.

16 November 1990; accepted 8 February 1991

Molecular Self-Assembly of Two-Terminal, Voltammetric Microsensors with Internal References

JAMES J. HICKMAN, DAVID OFER, PAUL E. LAIBINIS, GEORGE M. WHITESIDES, MARK S. WRIGHTON*

Self-assembly of a ferrocenyl thiol and a quinone thiol onto Au microelectrodes forms the basis for a new microsensor concept: a two-terminal, voltammetric microsensor with reference and sensor functions on the same electrode. The detection is based on measurement of the potential difference of current peaks for oxidation and reduction of the reference (ferrocene) and indicator (quinone) in aqueous electrolyte in a two-terminal, linear sweep voltammogram in which a counterelectrode of relatively large surface area is used. The quinone has a half-wave potential, $E_{1/2}$, that is pH-sensitive and can be used as a pH indicator; the ferrocene center has an $E_{1/2}$ that is a pH-insensitive reference. The key advantages are that such sensors require no separate reference electrode and function as long as current peaks can be located for reference and indicator molecules.

WE REPORT PROOF-OF-CONCEPT results demonstrating a new approach to electrochemical sensors: two-terminal, voltammetric microsensors with internal references (Fig. 1). Detection is accomplished by measurement of the potential difference, ΔE, associated with current peaks for oxidation (or reduction) of microelectrode-confined redox reagents, where the magnitude of ΔE can be related to the concentration of analyte. One of the electrode-bound reagents has an electrochemical response that is insensitive to variations in the medium and serves as the reference.At least one of the electrode-bound reagents is chemically sensitive and serves as the indicator. Current peaks for oxidation or reduction of the reference and indicator are determined from two-terminal, linear sweep voltammograms in which a counterelectrode is used that has an area

J. J. Hickman, D. Ofer, M. S. Wrighton, Department of Chemistry, Massachusetts Institute of Technology, Cambridge, MA 02139. P. E. Laibinis and G. M. Whitesides, Department of Chemistry, Harvard University, Cambridge, MA 02138.

*To whom correspondence should be addressed.